

Residual stress modeling of mitigated fused silica damage sites with CO_2 laser annealing

Chuanchao Zhang(张传超), Wei Liao(廖威), Lijuan Zhang(张丽娟), Xiaolong Jiang(蒋晓龙), Zhenhua Fang(方振华), and Xiaodong Jiang(蒋晓东)

Citation: Chin. Phys. B, 2024, 33 (**3**): 036101. DOI: 10.1088/1674-1056/acf447
Journal homepage: http://cpb.iphy.ac.cn; http://iopscience.iop.org/cpb

What follows is a list of articles you may be interested in

Thermal stress damage mechanism in single-crystal germanium caused by 1080 nm laser irradiation

Yin-Chuan Sha(沙银川), Ze-Wen Li(李泽文), Zhi-Chao Jia(贾志超), Bing Han(韩冰), and Xiao-Wu Ni(倪晓武)
Chin. Phys. B, 2023, 32 (**10**): 106104. DOI: 10.1088/1674-1056/acb41f

Boosting the performance of crossed ZnO microwire UV photodetector by mechanical contact homo-interface barrier

Yinzhe Liu(刘寅哲), Kewei Liu(刘可为), Jialin Yang(杨佳霖), Zhen Cheng(程祯), Dongyang Han(韩冬阳), Qiu Ai(艾秋), Xing Chen(陈星), Yongxue Zhu(朱勇学), Binghui Li(李炳辉), Lei Liu(刘雷), and Dezhen Shen(申德振)
Chin. Phys. B, 2022, 31 (**10**): 106101. DOI: 10.1088/1674-1056/ac80b0

Theoretical and experimental studies on high-power laser-induced thermal blooming effect in chamber with different gases

Xiangyizheng Wu(吴祥议政), Jian Xu(徐健), Keling Gong(龚柯菱), Chongfeng Shao(邵崇峰), Yang Kou(寇洋), Yuxuan Zhang(张宇轩), Yong Bo(薄勇), and Qinjun Peng(彭钦军)
Chin. Phys. B, 2022, 31 (**8**): 086105. DOI: 10.1088/1674-1056/ac6165

Sphere-shaped SiGe micro/nanostructures with tunable Ge composition and size formed by laser irradiation

Xinxin Li(李欣欣), Zhen Deng(邓震), Sen Wang(王森), Jinbiao Liu(刘金彪), Jun Li(李俊), Yang Jiang(江洋), Ziguang Ma(马紫光), Chunhua Du(杜春花), Haiqiang Jia(贾海强), Wenxin Wang(王文新), and Hong Chen(陈弘)
Chin. Phys. B, 2021, 30 (**9**): 096104. DOI: 10.1088/1674-1056/ac0347

Structural modification in swift heavy ion irradiated muscovite mica

Sheng-Xia Zhang(张胜霞), Jie Liu(刘杰), Jian Zeng(曾健), Pei-Pei Hu(胡培培), Peng-Fei Zhai(翟鹏飞)
Chin. Phys. B, 2017, 26 (**10**): 106102. DOI: 10.1088/1674-1056/26/10/106102

Residual stress modeling of mitigated fused silica damage sites with CO_2 laser annealing

Chuanchao Zhang(张传超)†, Wei Liao(廖威), Lijuan Zhang(张丽娟), Xiaolong Jiang(蒋晓龙), Zhenhua Fang(方振华), and Xiaodong Jiang(蒋晓东)

Laser Fusion Research Center, China Academy of Engineering Physics, Mianyang 621900, *China*

(Received 7 May 2023; revised manuscript received 9 August 2023; accepted manuscript online 28 August 2023)

A numerical model based on measured fictive temperature distributions is explored to evaluate the residual stress fields of CO_2 laser-annealed mitigated fused silica damage sites. The proposed model extracts the residual strain from the differences in thermoelastic contraction of fused silica with different fictive temperatures from the initial frozen-in temperatures to ambient temperature. The residual stress fields of mitigated damage sites for the CO_2 laser-annealed case are obtained by a finite element analysis of equilibrium equations and constitutive equations. The simulated results indicate that the proposed model can accurately evaluate the residual stress fields of laser-annealed mitigated damage sites with a complex thermal history. The calculated maximum hoop stress is in good agreement with the reported experimental result. The estimated optical retardance profiles from the calculated radial and hoop stress fields are consistent with the photoelastic measurements. These results provide sufficient evidence to demonstrate the suitability of the proposed model for describing the residual stresses of mitigated fused silica damage sites after CO_2 laser annealing.

Keywords: fused silica, damage mitigation, residual stress, laser annealing

PACS: 61.80.Ba, 63.50.Lm, 42.70.Ce, 78.20.–e **DOI:** 10.1088/1674-1056/acf447

1. Introduction

High-quality fused silica can be produced at large scales and is widely used for the manufacture of large and expensive optical components such as windows, lenses and gratings suitable for high-power laser systems. Over the past decades, despite significant progress having been made in increasing the damage resistance of fused silica optics operating at UV wavelengths, laser-induced surface damage of fused silica optics is still a major issue for high-power laser systems.[1–3] Although the surface damage sites initially have a diameter of the order of tens of microns, the size of such sites increases exponentially with subsequent high-fluence nanosecond UV laser shots, which limits the durability of optical components for high-power laser systems.[4,5] To avoid growth of the damage site, localized CO_2 laser melting of fused silica has been used to mitigate surface damage sites on fused silica optics.[6–9] However, thermal quenching following the melting of damage sites can accumulate a significant amount of residual stress due to the finite relaxation times near the glass transition of fused silica, which may cause critical fracture to relieve stress throughout the heat-treated region.[10] CO_2 laser annealing by a linear ramp-down of laser power after damage mitigation has been demonstrated and applied to avoid rapid cooling down, which minimizes the residual stress to an acceptable level, avoiding critical fracture.[11–13]

Accurate description of residual stress of mitigated fused silica damage sites for quenched and laser-annealed cases is of major interest for optimization of the damage mitigation process. The nondestructive photoelastic method is generally used to characterize stress in transparent materials. The measured retardance value is associated with the stress level to be evaluated. But the residual stress of mitigated damage sites is nonuniform, and there is no direct proportionality between the retardance and the stress level of a mitigated damage site. Thus, the stress distribution and quantitative values of stress levels of a mitigated fused silica damage site cannot be directly evaluated by the photoelastic method.[14] In order to assess the residual stress distribution of mitigated fused silica damage sites, various numerical models of CO_2 laser interaction with fused silica, which take into account multiphysics processes and temperature-dependent physical properties in the whole thermal history during localized CO_2 laser treatment of fused silica, have been developed to quantify the residual stress of mitigated damage sites. Gallais *et al.* regarded the residual stress of mitigated damage sites as the imprinted thermal stress induced by temperatures below a limit between 1100 °C and 1600 °C after heating.[14] Matthews *et al.* indicated that the magnitude of the final residual tensile stress of mitigated damage sites is nearly equal to the maximum compressive stress prior to cool-down.[12] Vignes *et al* presented a multiphysics finite-element model to analyze the residual stress of mitigated damage sites considering viscous flowing, quenching of the material and structural relaxation.[15] These reported numerical models have been successfully used to evaluate the residual stress distribution of quench-cooled mitigated damage sites. For CO_2 laser annealing, however, the mitigated

†Corresponding author. E-mail: zhchch@caep.cn

© 2024 Chinese Physical Society and IOP Publishing Ltd

damage site shows a more complex thermal history, meaning that the reported numerical models inaccurately predict the residual stress distribution of laser-annealed mitigated damage sites. Matthews *et al.* reported that the calculated value for the maximum hoop stress of mitigated damage sites with CO_2 laser annealing is 41% larger than the value from critical fracture experiments, while the deviation between the calculated and experimental values for the maximum hoop stress of quench-cooled mitigated damage sites is only 6%.[12] Hence, the ability to accurately assess the residual stresses of laser-annealed mitigated damage sites is still a challenge.

In this study, a numerical model based on the measured fictive temperature distribution of the mitigated damage sites is explored to evaluate the distribution and quantitative values of the residual stress of CO_2 laser-annealed mitigated fused silica damage sites. The fictive temperature of a glass, which is defined as the temperature of the equilibrium melt whose structure is equivalent to that of the cooled glass, is a convenient tool in describing glass structural relaxation phenomena.[16] The proposed model assumes that the initial frozen-in state of fused silica is the zero-point of residual stresses in the melt zone, and the generation of residual stresses results from the differences in thermoelastic contraction of fused silica with different fictive temperatures from the initial frozen-in temperature to ambient temperature, and has succeeded in evaluating the nonuniform residual stress fields of quench-cooled mitigated damage sites.[17] Spatially resolved fictive temperatures of mitigated damage sites for quenched and CO_2 laser-annealed cases have been widely characterized using confocal Raman microscopy.[12,18] Based on the reported fictive temperature distribution, the residual stress fields of the CO_2 laser-annealed mitigated damage sites were systematically analyzed by the proposed model in this study, and the calculated maximum hoop stress agrees well with the reported experimental result, demonstrating the suitability of the proposed model for describing the residual stresses of mitigated fused silica damage sites for CO_2 laser annealing.

2. Residual stress model based on fictive temperature

During the localized CO_2 laser melting of a fused silica damage site the melted fused silica is soft, and thermally induced stresses are released by structural relaxation. The melt zone persists in a zero-stress state until the laser is shut off, and rapid thermal quenching ensues. Due to the high cooling rate for the quenched case, the melt zone of the mitigated site is frozen-in at higher fictive temperatures with greater density. After collective cooling of fused silica, the melt zone undergoes intense residual tensile stresses, while CO_2 laser annealing by a linear ramp-down of laser power following damage mitigation can effectively suppress rapid cool-down and allow the melt zone to more fully relax. Thus, the mitigated damage site for the CO_2 laser-annealed case is frozen-in at a lower fictive temperature than for the quenched case, and therefore the residual stress is effectively minimized.[11–13] The axial fictive temperature distributions of mitigated damage sites for quenched and CO_2 laser-annealed cases have both been widely characterized.[12,18]

According to the reported data for mitigated damage sites quench-cooled at a peak temperature of 2300 K and mitigated damage sites laser-annealed by linear ramp from a maximum of 2300 K to ambient 300 K,[12] depth profiles of fictive temperatures on the axis of mitigated damage sites can be fitted as logistic curves

$$T_{\mathrm{f_{quenched}}}(z)_{\mathrm{on-axis}} = 1349.64 + \frac{511.93}{1+\left(\frac{z}{212.95}\right)^{6.45}}, \quad (1)$$

$$T_{\mathrm{f_{annealed}}}(z)_{\mathrm{on-axis}} = 1302.59 + \frac{377.82}{1+\left(\frac{z}{139.61}\right)^{2.67}}, \quad (2)$$

where $T_{\mathrm{f_{quenched}}}(z)_{\mathrm{on-axis}}$ (in K) is the depth profile of on-axis fictive temperatures of mitigated damage sites quench-cooled at 2300 K peak temperature, $T_{\mathrm{f_{annealed}}}(z)_{\mathrm{on-axis}}$ (in K) is the depth profile of on-axis fictive temperatures of mitigated damage sites laser-annealed by linear ramping from a maximum of 2300 K to ambient 300 K; z is measured in microns.

The two-dimensional (2D) axisymmetric fictive temperature distributions of mitigated damage sites result from isotropic thermal diffusion of the thermodynamic temperature field, and show an axisymmetric characteristic of a spherical cap.[17] Thus, the fictive temperature distributions can be mapped by the fictive temperature profiles along the axial depth. According to Eqs. (1) and (2) and the distribution characteristics of fictive temperatures for the mitigated damage sites in Ref. [17], the 2D axisymmetric fictive temperature distributions of mitigated damage sites can be described as

$$T_{\mathrm{f_{quenched}}}(r,z) = 1349.64 + \frac{511.93}{1+\left(\frac{\sqrt{r^2+(z+423)^2}-423}{212.95}\right)^{6.45}}, \quad (3)$$

$$T_{\mathrm{f_{annealed}}}(r,z) = 1302.59 + \frac{377.82}{1+\left(\frac{\sqrt{r^2+(z+423)^2}-423}{139.61}\right)^{2.67}}, \quad (4)$$

where $T_{\mathrm{f_{quenched}}}(r,z)$ is the 2D axisymmetric fictive temperature distribution of mitigated damage sites quench-cooled at 2300 K peak temperature, $T_{\mathrm{f_{annealed}}}(r,z)$ is the 2D axisymmetric fictive temperature distributions of mitigated damage sites laser-annealed by linear ramping from a maximum of 2300 K to ambient 300 K. The typical fictive temperature distributions of mitigated damage sites for both quenched and laser-annealed cases were artificially reconstructed according to Eqs. (3) and (4), and are shown in Fig. 1, where it can be seen that CO_2 laser annealing can effectively abate the local fictive temperature modification of mitigated damage sites.

Before damage mitigation, the fictive temperature of the fused silica substrate is uniform with a value of 1315 K. After damage mitigation, the fictive temperature of the local melt zone increases, as shown in Fig. 1, resulting in local densification and induction of tensile stresses on the surface of mitigated damage sites. The key of the proposed model for evaluating the residual stress of mitigated damage sites is that the relationship between residual strain and fictive temperature can be determined. According to the proposed model of residual stress fields analyzed from fictive temperature distributions for quench-cooled mitigated damage sites,[17] the difference between specific volume changes of fictive temperature-increased fused silica and the substrate from the initial frozen-in temperatures to the ambient temperature can be regarded as the residual thermal volume displacement as the body collectively cools. Therefore the residual thermal volume strain of fused silica with fictive temperature $T_{\rm f}$ is expressed as

$$\varepsilon_{\rm resid_vol}(T_{\rm f}) = \frac{[V(T_0,T_{\rm f}) - V(T_{\rm f},T_{\rm f})] - [V(T_0,T_{\rm f_ini}) - V(T_{\rm f_ini},T_{\rm f_ini})]}{V(T_0,T_{\rm f})}, \tag{5}$$

where $V(T,T_{\rm f}) = [1+3\alpha(T_{\rm f})(T-T_0)]/\rho(T_{\rm f})$ is the specific volume of fused silica with fictive temperature $T_{\rm f}$ at thermodynamic temperature T, $T_{\rm f_ini}$ is the initial fictive temperature of the fused silica substrate with a value of 1315 K and T_0 is room temperature.

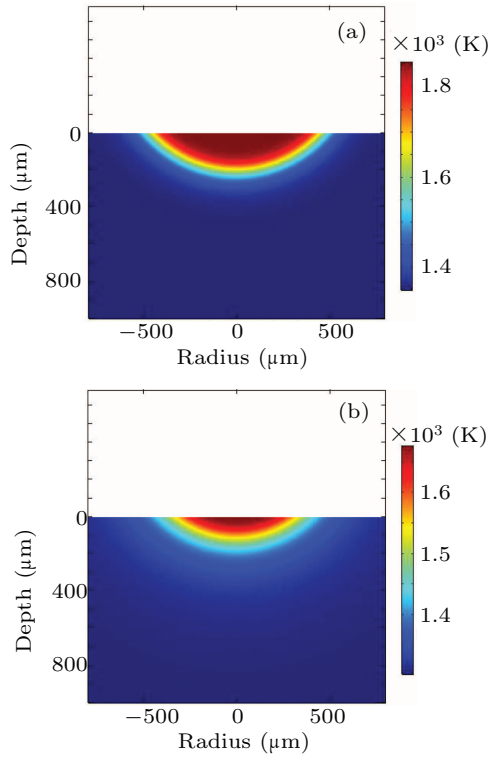


Fig. 1. The artificial reconstruction of typical fictive temperature distributions of mitigated damage sites in Ref. [12] for mitigated damage sites quench-cooled at a peak temperature of 2300 K (a) and mitigated damage sites laser-annealed by linear ramping from a maximum of 2300 K to ambient 300 K (b).

According to the symmetry of this study, a 2D axisymmetric geometry is used to describe the residual stress as a function of the residual thermal strain of fictive temperature-increased fused silica. Making use of the cylindrical coordinate system (r, θ, z) for axially symmetric problems,[19] the constitutive equations for the axisymmetric fictive temperature modification zone of mitigated damage sites are as follows:

$$\begin{aligned}
\varepsilon_{rr} &= \frac{1}{E}[\sigma_{rr} - \nu(\sigma_{\theta\theta}+\sigma_{zz})] + \frac{1}{3}\varepsilon_{\rm resid_vol}(T_{\rm f}),\\
\varepsilon_{\theta\theta} &= \frac{1}{E}[\sigma_{\theta\theta} - \nu(\sigma_{zz}+\sigma_{rr})] + \frac{1}{3}\varepsilon_{\rm resid_vol}(T_{\rm f}),\\
\varepsilon_{zz} &= \frac{1}{E}[\sigma_{zz} - \nu(\sigma_{rr}+\sigma_{\theta\theta})] + \frac{1}{3}\varepsilon_{\rm resid_vol}(T_{\rm f}),\\
\varepsilon_{zr} &= \frac{\sigma_{zr}}{2G},
\end{aligned} \tag{6}$$

where the ε values are components of the strain, E is Young's modulus, G is shear modulus and ν is Poisson's ratio.

Combining the equilibrium equations and constitutive equations, the residual stresses of mitigated damage sites for laser annealing can be obtained by commercial finite element analysis (FEA) software. The physical properties of fused silica used in the model are summarized in Table 1.

Table 1. Physical properties of fused silica used in the calculations.

Property	Symbol	Value
Density (kg·m^{-3})	$\rho(T_{\rm f})$	$0.001T_{\rm f}+2186.7$[a)]
Thermal expansion coefficient (K^{-1})	$\alpha(T_{\rm f})$	$[0.267+2.88\times10^{-4}(T_{\rm f}-273.15)$ $-3.26\times10^{-5}\times900]\times10^{-6}$[b)]
Young's modulus (GPa)	$E(T_{\rm f})$	$\rho(T_{\rm f})\times(5859.52+0.07216T_{\rm f})$[2a)]
Poisson's ratio	ν	0.16

[a)]Ref. [2], [b)]Ref. [3].

3. Results and discussion

From Eqs. (3)–(6) and the equations of equilibrium for axially symmetric problems

$$\begin{aligned}
\frac{\partial\sigma_{rr}}{\partial r} + \frac{\partial\sigma_{zr}}{\partial z} + \frac{\sigma_{rr}-\sigma_{\theta\theta}}{r} &= 0,\\
\frac{\partial\sigma_{rz}}{\partial r} + \frac{\partial\sigma_{zz}}{\partial z} + \frac{\sigma_{rz}}{r} &= 0,
\end{aligned} \tag{7}$$

where the σ are components of the stress, the residual stress field of a mitigated damage site can be obtained by solving elastic equilibrium conditions and stress–strain relations.

The calculated hoop stress fields of mitigated damage sites for quenched and CO_2 laser-annealed cases based on fic-

tive temperature distributions are shown in Fig. 2, which indicates that the local fictive temperature modification zones of mitigated damage sites suffer intensive tensile stress. For the mitigated damage sites quench-cooled at a peak temperature of 2300 K, the hoop stresses remain almost constant on the melt surface. The hoop stress at the surface center $r = 0$ is 21.8 MPa and increases slowly to a maximum of 23.7 MPa at $r = 335$ μm; with the radius further increasing, the hoop stress decreases rapidly and reaches a minimum of −2.4 MPa at $r = 660$ μm. For the mitigated damage sites laser-annealed by linear ramping from a maximum of 2300 K to ambient 300 K, the hoop stresses are almost constant at the melt surface center, and the hoop stress at the surface center $r = 0$ is 16.8 MPa and just slowly increases to a maximum of 17.2 MPa at $r = 150$ μm; with the radius further increasing, the hoop stress gradually decreases to 0 at $r = 650$ μm. In comparison with the calculated hoop stresses at the melt surface center for quenched and CO_2 laser-annealed cases, CO_2 laser annealing can effectively suppress the maximum surface hoop stress.

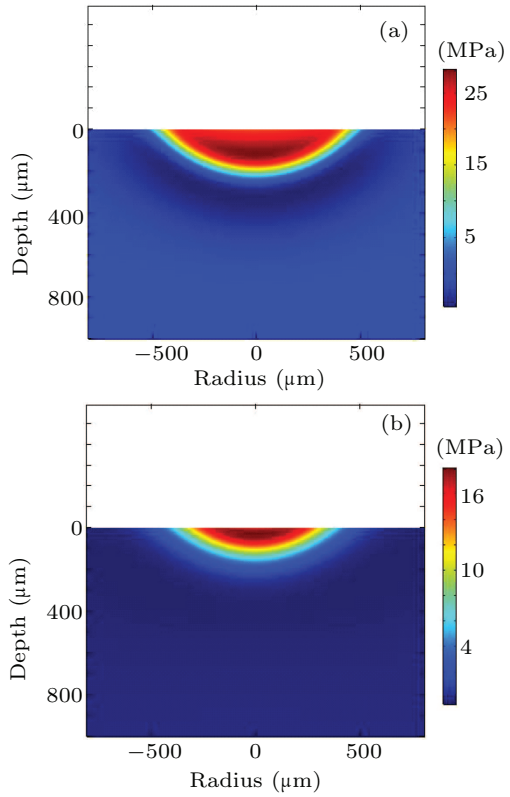


Fig. 2. Calculated hoop stresses $\sigma_{\theta\theta}$ of mitigated damage sites for mitigated damage sites quench-cooled at a peak temperature of 2300 K (a) and mitigated damage sites laser-annealed by linear ramping from a maximum of 2300 K to ambient 300 K (b). A positive value for the stress indicates tension.

On the axis, the tensile hoop stresses of quench-cooled mitigated damage sites dramatically increase from 21.8 MPa at $z = 0$ to a maximum of 28.4 MPa at $z = 110$ μm, and then rapidly decrease to −4.5 MPa at $z = 330$ μm. The axial tensile hoop stresses of laser-annealed mitigated damage sites increase from 16.8 MPa at $z = 0$ to a maximum of 18.1 MPa at $z = 35$ μm, and then gradually decrease to 0 at $z = 280$ μm. It is interesting to note that the maximum hoop stresses of quench-cooled mitigated damage sites do not occur at $z = 0$ on-axis, but in fact reside in regions below the surface at $z = 110$ μm, which is consistent with the results in Ref. [12]. The maximum hoop stress of quench-cooled mitigated damage sites is 57% larger than that of laser-annealed mitigated damage sites.

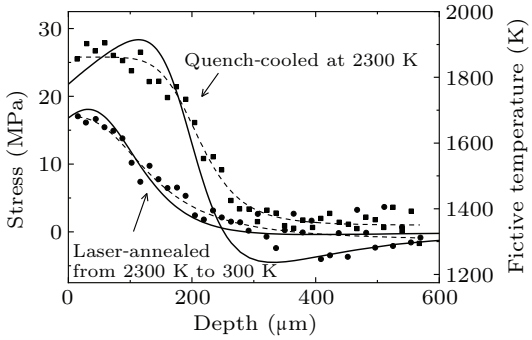


Fig. 3. Depth profiles of the calculated hoop stress $\sigma_{\theta\theta}$ along the axis of mitigated damage sites for quenched and CO_2 laser annealed cases (solid line). The fictive temperature profiles on the axis used in the calculations are plotted for comparison (dashed line). Square and circle symbols are data points in Ref. [12].

The depth profiles of fictive temperatures and calculated hoop stresses on the axis of mitigated damage sites for quenched and CO_2 laser-annealed cases are plotted in Fig. 3 for comparison. The quenched and laser-annealed cases both display a characteristic sigmoidal shape with nearly constant T_f at the surface, and a mostly monotonic decrease into the bulk to T_{f_ini}. It is obvious that the hoop stresses increase to the maximum value with depth of constant T_f increasing, and then decrease with the decrease of fictive temperatures. The slopes of hoop stresses are consistent with those of the corresponding fictive temperatures for quenched and CO_2 laser-annealed cases. According to the reported depth profiles of fictive temperatures for thermally quenched silica sites at peak temperatures of 1700 K and 2300 K in Ref. [12], the maximum hoop stresses for the mitigated damage sites quench-cooled at peak temperatures of 1700 K and 2300 K are also calculated by the proposed model. The calculated maximum hoop stresses in this study and the calculated and measured maximum hoop stresses in Ref. [12] are summarized in Table 2. The second column indicates maximum hoop stresses estimated from critical fracture experiments in Ref. [12]. The third column indicates maximum hoop stresses simulated by the finite element analysis of the model in Ref. [12]. The fourth column indicates calculated maximum hoop stresses using the proposed model in this work.

For the quenched case at a peak temperature of 1700 K, the maximum hoop stress 16.8 MPa calculated by the proposed model in this study is consistent with the experimental result of $<$ 18.7 MPa in Ref. [12], while the calculated

maximum hoop stress of 26.7 MPa in Ref. [12] is much larger than the experimental result. For the quenched case at a peak temperature of 2300 K, both the simulated maximum hoop stresses in Ref. [12] and in this work are close to the experimental results, which indicates that the models used in Ref. [12] and in this work can both effectively evaluate the residual stress fields of mitigated damage sites quench-cooled at a peak temperature of 2300 K. Compared with the maximum hoop stresses for thermally quenched mitigated damage sites at 1700 K, 2300 K and 3000 K calculated using the proposed model, it is obvious that the maximum hoop stresses increase with increasing quenched peak temperature, which agrees with the general experimental results.

Table 2. Summary of calculated and measured maximum hoop stresses.

Case	σ_c (MPa) from Ref. [12]	σ_{FEA}, max (MPa) from Ref. [12]	σ_{FEA}, max (MPa) (this work)
Quench-cooled at 1700 K	$< 18.7 \pm 0.5$	26.7	16.8
Quench-cooled at 2300 K	29 ± 3.1	30.6	28.4
Quench-cooled at 3000 K	–	–	33.6
Laser-annealed from 2300 K to 300 K	19 ± 1.3	26.8	18.1

For the laser-annealed case, the calculated maximum hoop stress in Ref. [12] is 41% larger than the experimental result, while the calculated maximum hoop stress in this study is just 5% less than the experimental result. Thus, the proposed model in this study can accurately evaluate the residual stress fields of mitigated damage sites for the laser-annealed case. The residual stress generation of mitigated damage sites is a multiphysics process involving viscous flowing, quenching of the material and structural relaxation. In addition, the physical properties of fused silica are temperature dependent. Thus, it is extremely difficult to precisely assess the residual stress directly from the thermal history of the localized CO_2 laser treatment of fused silica. The proposed model is just dependent on the measured fictive temperature distribution, and avoids complex thermodynamic processes. Therefore, the proposed model can accurately evaluate the residual stress fields of laser-annealed mitigated damage sites with a more complex thermal history.

The calculated radial stress fields of mitigated damage sites for quenched and CO_2 laser-annealed cases based on fictive temperature distributions are shown in Fig. 4. The distributions of radial stresses are significantly different from those of hoop stresses. The tensile radial stresses on the surface extend far beyond the local fictive temperature modification zone. For the mitigated damage sites quench-cooled at a peak temperature of 2300 K, the surface radial stresses rapidly increase from 21.8 MPa at $r = 0$ to a maximum of 35.8 MPa at $r = 335$ μm, and then gradually decrease to zero at radii larger than 2 mm. For the mitigated damage sites laser-annealed by linear ramping from a maximum of 2300 K to ambient 300 K, the radial stresses just slowly increase from 16.8 MPa at $r = 0$ to a maximum of 19.5 MPa at $r = 245$ μm, and then gradually decrease to zero at radii larger than 2 mm. Compared with the fictive temperature distributions in Fig. 1, the maximum residual radial stresses reside in the border regions of local fictive temperature modification zones, where the slope of the fictive temperature profiles is larger. The maximum radial stress of quench-cooled mitigated damage sites is 84% larger than that of laser-annealed mitigated damage sites, which shows that CO_2 laser annealing can effectively suppress the maximum radial stress.

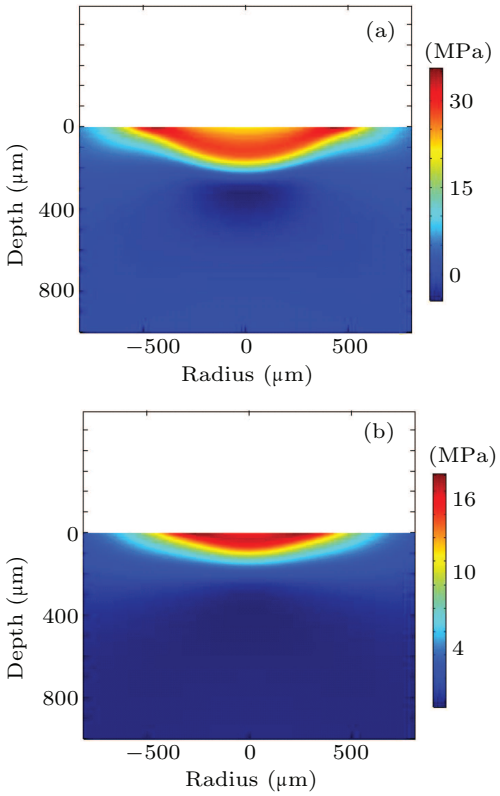


Fig. 4. Calculated radial stresses σ_{rr} of mitigated damage sites for mitigated damage sites quench-cooled at a peak temperature of 2300 K (a) and mitigated damage sites laser-annealed by linear ramping from a maximum of 2300 K to ambient 300 K (b). A positive value for the stress indicates tension.

According to the residual radial and hoop stress fields, it is convenient to assess the optical retardance caused by stress-induced birefringence. The calculated residual radial and hoop stress fields have an azimuthal symmetry. The directions of principal stresses are parallel or orthogonal to the radius. The relative optical retardation between waves polarized in the radial direction and in the tangential direction can be obtained by

the integrated principal stress difference along the z direction in this study, and can be calculated by[17,22]

$$R = \int_0^d K(\sigma_{rr} - \sigma_{\theta\theta})\,\mathrm{d}z, \tag{8}$$

where K is the stress-optic coefficient of fused silica and is equal to 35 nm·cm^{-1}·MPa^{-1}, and d is the thickness of fused silica sample.

Figure 5 shows the radial profiles of optical retardance for a light beam traveling through the thickness of mitigated damage sites for quenched and laser annealed cases, which are calculated from the simulated residual hoop and radial stress fields in Figs. 2 and 4. The radial characteristic shape of the optical retardance for quench-cooled mitigated damage sites is in agreement with the reported measurement.[23] CO_2 laser annealing can effectively reduce the optical retardance of mitigated damage sites. The slope of the radial optical retardance profile of the laser-annealed mitigated damage sites dramatically decreases compared with that of quench-cooled mitigated damage sites.

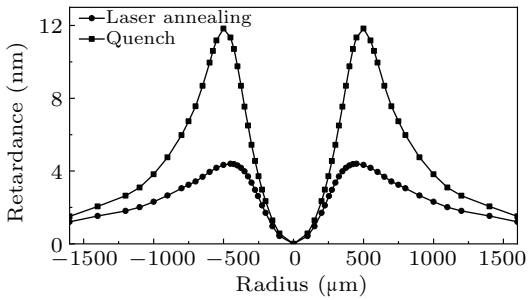


Fig. 5. The calculated radial profiles of optical retardance for a light beam traveling through the thickness of mitigated damage sites induced by the simulated residual radial and hoop stress fields for quenched and laser-annealed cases.

4. Conclusion

A numerical model based on the measured fictive temperature distribution of mitigated damage sites is explored to evaluate the quantitative values of the residual stress fields of CO_2 laser-annealed mitigated fused silica damage sites. The proposed model extracts the residual strain from the differences in thermoelastic contraction of fused silica with different fictive temperatures from initial frozen-in temperatures to the ambient temperature, and the residual stress fields of mitigated damage sites for the quenched and CO_2 laser-annealed cases are obtained by a finite element analysis of equilibrium equations and constitutive equations. The simulated results indicate that the proposed model can accurately evaluate the residual stress fields of laser-annealed mitigated damage sites with a more complex thermal history. The calculated maximum hoop stress is in good agreement with reported experimental results. The maximum hoop stress of quench-cooled mitigated damage sites is 57% larger than that of laser-annealed mitigated damage sites. The maximum radial stress of quench-cooled mitigated damage sites is 84% larger than that of laser-annealed mitigated damage sites. CO_2 laser annealing can effectively suppress the maximum residual stresses. The estimated optical retardance profiles from the calculated radial and hoop stress fields are consistent with photoelastic measurements. These results provide sufficient evidence to demonstrate the suitability of the proposed model to describe the residual stresses of mitigated fused silica damage sites for CO_2 laser annealing.

Acknowledgement

Project supported by the National Natural Science Foundation of China (Grant No. 62275235).

References

[1] Campbell J H, Hawley-Fedder R A, Stolz C J, Menapace J A, Borden M R, Whitman P K, Yu J, Runkel M, Riley M O, Feit M D and Hackel R P 2004 *Proc. SPIE* **5341** 84
[2] Han W, Huang W Q, Wang F, Li K Y, Feng B, Li F Q, Jing F and Zheng W G 2010 *Chin. Phys. B* **19** 106105
[3] Fleurot N, Cavailler C and Bourgade J L 2005 *Fusion Eng. Des.* **74** 147
[4] Norton M A, Adams J J, Carr C W, Donohue E E, Feit M D, Hackel R P, Hollingsworth W G, Jarboe J A, Matthews M J, Rubenchik A M and Spaeth M L 2007 *Proc. SPIE* **6720** 67200
[5] Chai X X, Li P, Zhao J P, Wang G Z, Zhu D Y, Jiang Y L, Chen B, Zhu Q H, Feng B, Wang L Q and Jing Y K 2021 *Optik* **226** 165549
[6] Palmier S, Gallais L, Commandre M, Cormont P, Courchinoux R, Lamaignere L, Rullier J L and Legros P 2009 *Appl. Surf. Sci.* **255** 5532
[7] Adams J J, Bolourchi M, Bude J D, Guss G M, Matthews M J and Nostrand M C 2010 *Proc. SPIE* **7842** 784223
[8] Mendez E, Nowak K M, Baker H J, Villarreal F J and Hall D R 2006 *Appl. Opt.* **45** 5358
[9] Jiang Y, Liu C M, Luo C S, Yuan X D, Xiang X, Wang H J, He S B, Lü H B, Ren W, Zheng W G and Zu X T 2012 *Chin. Phys. B* **21** 054216
[10] Jiang Y, Xiang X, Liu C M, Wang H J, Liao W, Lv H B, Yuan X D, Qiu R, Yang Y J, Zheng W G and Zu X T 2015 *J. Non-Cryst. Solids* **410** 88
[11] Feit M D, Matthews M J, Soules T F, Stolken J S, Vignes R M, Yang S T and Cooke J D 2010 *Proc. SPIE* **7842** 78420
[12] Matthews M J, Stolken J S, Vignes R M, Norton M A, Yang S, Cooke J D, Guss G M and Adams J J 2009 *Proc. SPIE* **7504** 750410
[13] Zhang C C, Liao W, Zhang L J, Ye Y Y, Chen J, Wang H J, Luan X Y and Yuan X D 2014 *Adv. Cond. Matter Phys.* **2014** 638045
[14] Gallais L, Cormont P and Rullier J L 2009 *Opt. Express* **17** 23488
[15] Vignes R M, Soules T F, Stolken J S, Settgast R R, Elhadj S and Matthews M J 2013 *J. Am. Ceram. Soc.* **96** 137
[16] Scherer G W 1990 *J. Non-Cryst. Solids* **123** 75
[17] Zhang C C, Chen Q, Liao W, Dai R C, Zhang L J, Jiang X L, Chen J, Zhang Z M and Jiang X D 2021 *Opt. Express* **29** 42511
[18] Matthews M J, Vignes R M, Cooke D, Yang S T and Stolken J S 2010 *Opt. Lett.* **35** 1311
[19] Noda N, Hetnarski R B and Tanigawa Y 2003 *Thermal stresses*, 2nd edn. (New York: Taylor & Francis) p. 259
[20] Le Parc R, Levelut C, Pelous J, Martinez V and Champagnon B 2006 *J. Phys.: Condens. Matter* **18** 7507
[21] Kühn B and Schadrack R 2009 *J. Non-Cryst. Solids* **355** 323
[22] Horn G, Lesniak J, Mackin T and Boyce B 2005 *Rev. Sci. Instrum.* **76** 045108
[23] Yang L, Liao W, Miao X X, Yuan X D, Zheng W G, Lv H B, Zhou G R, Zu X T and Xiang X 2015 *Opt. Eng.* **54** 057105